Agricultural and Forest Meteorology 151 (2011) 916–926

Contents lists available at ScienceDirect

Agricultural and Forest Meteorology

journal homepage: www.elsevier.com/locate/agrformet

Tracking the structural and functional development of a perennial pepperweed (*Lepidium latifolium* L.) infestation using a multi-year archive of webcam imagery and eddy covariance measurements

O. Sonnentag[a,b,*], M. Detto[a,1], R. Vargas[a,c,1], Y. Ryu[a,b,1], B.R.K. Runkle[d,e], M. Kelly[a,1], D.D. Baldocchi[a,1]

[a] University of California Berkeley, Department of Environmental Science, Policy and Management, 137 Mulford Hall #3115, Berkeley, CA 94720, USA
[b] Harvard University, Department of Organismic and Evolutionary Biology, 22 Divinity Avenue, Cambridge, MA 02138, USA
[c] Departamento de Biología de la Conservación, Centro de Investigación Científica y de Educación Superior de Ensenada (CICESE), Ensenada, BC, Mexico
[d] University of California Berkeley, Department of Civil and Environmental Engineering, 760 Davis Hall #1710, Berkeley, CA 94720, USA
[e] University of Hamburg, Department of Soil Science, Allende-Platz 2, 20146 Hamburg, Germany

ARTICLE INFO

Article history:
Received 19 November 2010
Received in revised form 18 February 2011
Accepted 21 February 2011

Keywords:
Pepperweed
Near-surface remote sensing
Digital camera imagery
Canopy photosynthesis
Surface roughness length
Invasive plants

ABSTRACT

The continued spread of invasive weeds is threatening ecosystem health throughout North America. Understanding the relationships between invasive weeds' key phenological phases and structural and/or functional canopy development is an essential step for making informed decisions regarding their management. We analyzed a three-year image archive obtained from an inexpensive webcam overlooking a perennial pepperweed (*Lepidium latifolium* L.) infestation in California to explore the ability of red (R)–green (G)–blue (B) color space information to track the structural and functional development of the pepperweed. We characterized structural and functional canopy development through surface roughness length (z_{0m}; a proxy for canopy height and leaf area index) and canopy photosynthesis (F_A), respectively, both of which we derived from eddy covariance measurements. Here we demonstrate the use of cross-correlation functions to determine the temporal lags between chromatic coordinates and two color indices, all calculated from *RGB* brightness levels, with z_{0m} and F_A. We found that these color metrics fail to represent the structural and/or functional state of the canopy. In contrast, *relative luminance* (*CIE Y*) appears to be a better indicator for z_{0m} and especially for F_A. We calculated *CIE Y* from pepperweed *RGB* brightness levels in relation to hypothetical horizontal reference *RGB* brightness levels. We obtained the latter by applying the ratio between horizontally measured and hypothetical incoming solar radiation on a vertical surface to *RGB* brightness levels of a vertically oriented reference of invariant light-grey color. We conclude that webcam image archives may provide an inexpensive tool for making informed decisions regarding the timing but not for assessing the effectiveness of invasive plant control measures such as mowing.

© 2011 Elsevier B.V. All rights reserved.

1. Introduction

Perennial pepperweed (*Lepidium latifolium* L.) is an aggressive invasive weed that has become a major ecological and economical problem in all western states of the United States and in several provinces (Alberta; British Columbia) of Canada (Francis and Warwick, 2007). For example, the infestation of pastures and hay meadows has resulted in decreased forage quality and, consequently, in unmarketable hay (Francis and Warwick, 2007; Young et al., 1995). Various control measures such as grazing and spring mowing have been employed to minimize the spread of pepperweed (Francis and Warwick, 2007). The application of herbicides to control pepperweed was found to be more effective for resprouting plants after spring mowing at the onset of flowering, resulting in increased basal leaf area compared to unmowed plants with higher steam leaf area (Renz and DiTomaso, 2004). Thus, the application of these control measures requires knowledge of pepperweed's structural (e.g., leaf area index) and/or functional (e.g., canopy photosynthesis) development to determine the timing of their application but also to assess their effectiveness (both leaf area index and canopy photosynthesis may serve as indicators for pepperweed biomass).

The relationship between a pepperweed canopy's structural and functional development and the plant's phenological cycle is complex: after germination plants grow large dark-green basal rosette

* Corresponding author at: University of California Berkeley, Department of Environmental Science, Policy and Management, 137 Mulford Hall #3115, Berkeley, CA 94720, USA. Tel.: +1 510 642 2874; fax: +1 510 643 5089.
E-mail address: oliver.sonnentag@gmail.edu (O. Sonnentag).
[1] Tel.: +1 510 642 2874; fax: +1 510 643 5089.

0168-1923/$ – see front matter © 2011 Elsevier B.V. All rights reserved.
doi:10.1016/j.agrformet.2011.02.011

leaves (maximum 30 cm long and maximum 8 cm wide; Francis and Warwick, 2007) oriented parallel to the ground surface. After a few weeks, vertical grey-green stems and associated smaller grey-green stem leaves (maximum 9 cm long and maximum 4.5 cm wide; Francis and Warwick, 2007) start to grow and the basal rosette leaves senescence. With continued growth, plants start to flower during secondary inflorescence and the canopy is characterized by a dense arrangement of small white flowers (sepals [leaf-like structures, together forming the calyx that protects the corolla of a flower]: ~1.2 × 08 mm, petals [colorful, leaf-like structures, together forming the corolla of a flower]: ~2.1 × 11 mm; see Francis and Warwick, 2007). Plants are generally fully grown before the canopy reaches peak bloom. After a prolonged flowering phase over several months, the plants reach seed maturation for several weeks before they start to senesce (Francis and Warwick, 2007). Canopy photosynthesis increases rapidly with the growth of basal rosette leaves and later stem leaves, but drops substantially due to flowering before the plants are fully grown (Sonnentag et al., 2011).

The timing of pepperweed germination, early vegetative growth, flowering, seed maturation, and senescence in the western United States has been broadly described based on field observations of vegetation status (i.e., *germination*: ~late-February–March, *vegetative growth* consisting of *early vegetative growth*: ~April–early-May and *flowering*: ~mid-May–August, *seed maturation*: ~September–mid-October, *senescence*: ~late-October–November, *dormancy*: ~December–mid-February; after Andrew and Ustin (2008). Pepperweed's phenological cycle is associated with characteristic changes in canopy color (Fig. 1), thus tracking the structural and functional development of a pepperweed canopy simply by continuous observations of its color is appealing. In addition, increased understanding of invasive plant phenology is needed to better understand invasive plant species' success and to develop effective management strategies (Godoy et al., 2009; Wolkovich and Cleland, 2010).

A series of studies have demonstrated that "near-surface" remote sensing based on light emitting diodes, photodiodes or digital cameras has the potential to overcome the limitations of field observations by individuals (e.g., logistics and lack of consistency, continuity and objectivity) for species-level vegetation monitoring (e.g., Garrity et al., 2010; Richardson et al., 2009; Ryu et al., 2010a). Most digital cameras used for this purpose have a native capture system in the Cartesian red (R)–green (G)–blue (B) color space, where *RGB* digital numbers (DN) represent brightness levels of the red, green and blue primary colors. These *RGB* DNs are derived from the spectral radiance recorded by the camera sensor over overlapping red, green blue wavelengths (i.e., over the visible part of the electromagnetic spectrum). However, the relative spectral response of the respective camera sensor is usually not available to the end-user, thus radiometric quantities and consequently spectral reflectance at different visible wavelengths cannot be easily retrieved from *RGB* DNs.

For visual inspection of a photograph in the *RGB* color space, each present color is represented by a combination of *RGB* brightness levels. In addition to visual inspection, digital photographs allow the separate extraction of color (brightness) information as *RGB* DNs for quantitative analysis of vegetation status. It needs to be emphasized that the *RGB* color space is well suited for color display purposes, and thus for visual inspection, but less so for quantitative analysis because the three *RGB* color space components are highly correlated (i.e., all three components change accordingly with changes in illumination intensity; see Cheng et al., 2001).

Generally speaking, *brightness* is a subjective concept depending on the individual observer and was defined by the *Commission International de L'Eclairage* (CIE; http://www.cie.co.at/) as "the attribute of visual sensation according to which an area appears to exhibit more or less light". To overcome the qualitative nature of *brightness*, CIE defined an objective quantity related to *brightness*, called *luminance* (*L*; candela [cd] m^{-2}, i.e., the luminous intensity per unit area of light emitted or reflected by a surface in a given direction). For practical reasons, *luminance* is often normalized relative to a specified white reference (RGB_{ref}), resulting in *relative luminance* (*CIE Y*) with values from 0 to 1 (Poynton, 2003).

A popular way to synthesize *RGB* color space information obtained from digital camera photographs is through color indices, i.e. algebraic combinations of *RGB* brightness levels such as *excess green* (Richardson et al., 2007; Woebbecke et al., 1995). *Excess green* was formulated as $2 \times G - (R + B)$ based on the finding that especially the green component of the *RGB* color space was useful to maximize the contrast between green plant and different background materials by enhancing the green component while minimizing the red and blue components (Woebbecke et al., 1995). The value range of *excess green* depends mainly on the imaging sensor (e.g., bit depth, color balance) and to a lesser extent on illumination intensity, and thus on the color characteristics of the resulting photographs. As a consequence, the direct comparison of absolute values of *excess green* from different digital cameras is difficult.

Over the last two decades, several *RGB* color indices have been formulated and explored especially in the horticultural and agricultural literature (e.g., Adamsen et al., 1999, 2000; Meyer and Camargo Neto, 2008; Perez et al., 2000; Woebbecke et al., 1995). Based on manually taken nadir photographs of individual plants, the goal of many of these studies was to improve distinctions between green plants and soil/residue background prior to image binarization (Perez et al., 2000; Woebbecke et al., 1995). In addition, other specific *RGB* color indices have been used throughout different environmental disciplines to track certain color changes and these might be transferable to detect color changes associated with pepperweed's phenological cycle. For example, Goddijn-Murphy et al. (2009) used a *blue–green ratio* to track *yellow* substance in digital photographs taken below the water surface.

Recently, digital cameras, especially those taking repeated horizontal or oblique photographs of the landscape at high temporal frequencies (several photographs per day) over time have obtained increased attention. Most of these ecosystem-scale studies used *excess green* to determine phenologically relevant dates and rates such as leaf emergence and green-up, respectively, for non-managed ecosystems (e.g., Ahrends et al., 2009; Jacobs et al., 2009; Kurc and Benton, 2010; Graham et al., 2010a; Richardson et al., 2009). Furthermore, a large number of spatially distributed high-frequency archives of landscape photographs allows for detailed land surface characterization over time, and thus may play an important role for remote sensing product evaluation and refinement (Graham et al., 2010a; Jacobs et al., 2009).

Here we report on the application of a multi-year image archive (October 2007–October 2010) obtained from an inexpensive webcam (<$100 USD) overlooking a grazed peatland pasture that is infested by perennial pepperweed (*L. latifolium* L.). The goal was to explore the ability of *RGB* color space information from webcam imagery to track the structural and functional development of the pepperweed infestation for making informed decisions regarding its management. During the study period the site was subjected to year-round grazing and mowed once in 2008 (day-of-year [DOY] 137) early during flowering as widely applied measure to control pepperweed. The mowing event allowed us to see if a webcam image archive can be used as an aid to make decisions regarding the timing of a mowing event, and as an indicator for its effectiveness.

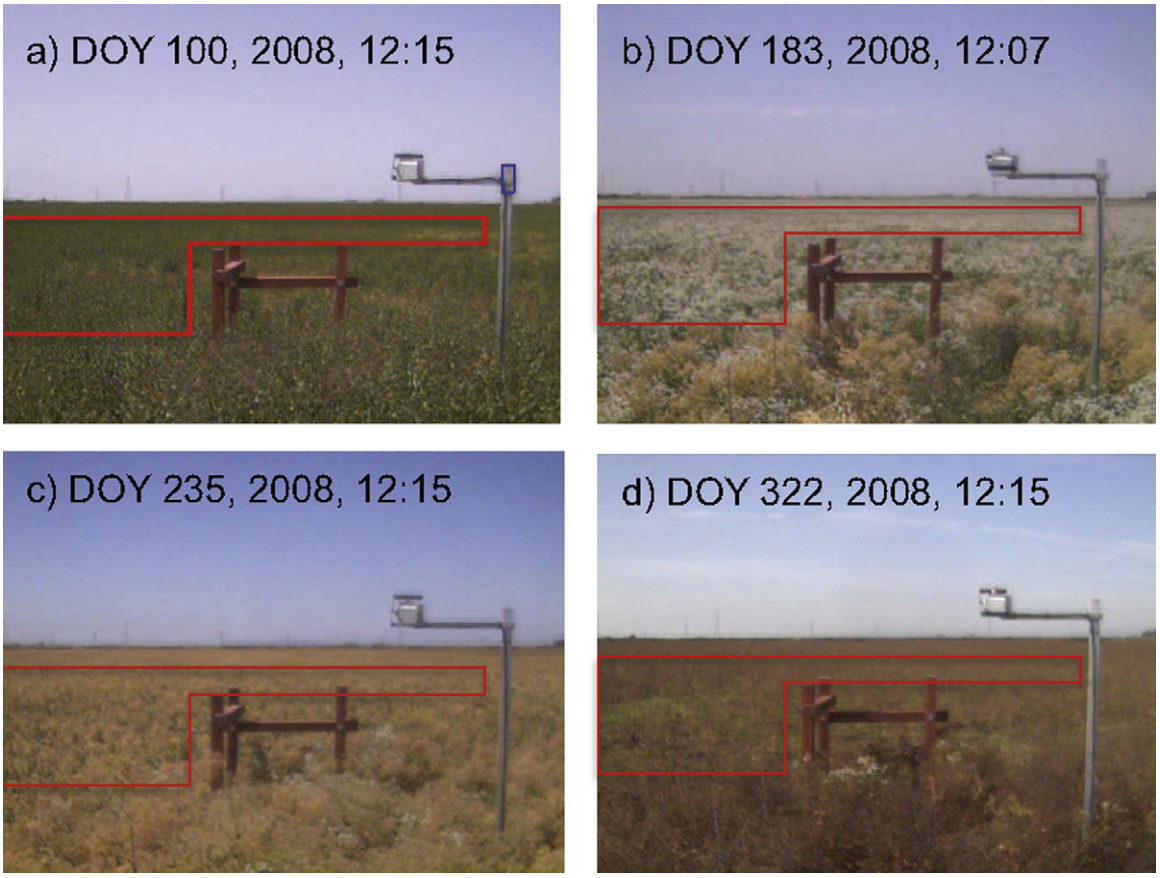

Fig. 1. Example webcam photographs for different pepperweed phenological phases: (a) early vegetative growth (green), (b) flowering (white), (c) seed maturation (yellow), and (d) senescence (brown). The red region-of-interest [ROI] delineates the region for which mean *RGB* brightness levels were extracted. The blue ROI was used to extract *RGB* brightness levels for the light-grey instrumentation pole and used on the calculation of relative luminance (Y). For temporal location of (a)–(d) see Fig. 3c. (For interpretation of the references to color in this figure legend, the reader is referred to the web version of the article.)

2. Methods

2.1. Study site

Our study site ($\sim 0.9 \times \sim 0.4 = \sim 0.36\,km^2$) is a grazed peatland pasture infested by pepperweed on Sherman Island (latitude: 38.0367°N; longitude: 121.7540°W; elevation: 7 m below sea level) in California's Sacramento-San Joaquin River Delta, about 60 km east of San Francisco. The climate of the area is classified as Mediterranean with dry, hot summers and wet, cool winters. Mean annual precipitation at the site is 325 mm and mean annual air temperature is 15.1 °C (1949–1999 for Antioch climate station ~10 km south-west of Sherman Island).

The site is relatively flat and bounded and dissected by land management ditches that are part of a delta-wide network of dikes, waterways and levees to regulate water flow across the landscape. The northern part of the site is characterized by a patchy ground cover of short (maximum 0.1 m) invasive annual C_3 grass (mouse barley; *Hordeum murinum* L.). The southern part is almost entirely infested by pepperweed (maximum height 1 m), which has been growing at the site for more than 20 years over a patchy grass ground cover (Juan Mercado [land manager], *personal communication*). The site was subjected to year-round grazing by beef cattle (~100, i.e. 278 km^{-2}), causing a discontinuous, open pepperweed canopy of varying height (maximum 1 m) and density over bare soil and small patches of short grass (Ryu et al., 2010b). During the study period the site was mowed once in early May 2008 (day-of-year [DOY] 137) as a control measure to reduce the reproductive success of pepperweed.

2.2. Eddy covariance and incoming solar radiation

In April 2007, we installed a micrometeorological tower located within a fenced enclosure in the southern part of the site to measure canopy gas and energy exchanges using eddy covariance (Baldocchi, 2003). Details on the measurements and the data post-processing are described elsewhere (Detto et al., 2010). The eddy covariance data was subjected to strict quality control and assurance criteria (Detto et al., 2010; Sonnentag et al., 2011). Vegetation canopy functioning as described by canopy photosynthesis (F_A) is closely related to canopy light interception and the light available within the canopy, both of which are a function of canopy structure and thus leaf area index. Daily integrated canopy photosynthesis (F_A; $g\,C\,m^{-2}\,d^{-1}$) was derived from half-hourly net ecosystem CO_2 exchange (F_C; $\mu mol\,m^{-2}\,s^{-1}$). Incoming solar radiation (S_g) was measured using a pyranometer with a spectral response from 305 to 2800 nm (CNR3, Kipp and Zonen, Delft, the Netherlands), logged by data loggers (CR10; Campbell Scientific, Logan, UT, USA) at 5 s intervals, and recorded as half-hourly mean values.

We used surface roughness length (z_{0m}; m) as a proxy to describe changes in pepperweed's structural canopy development (Sonnentag et al., 2011). Surface roughness length is the height above the ground surface where mean wind speed extrapolates to zero (Monteith and Unsworth, 1990), and it governs the rate that momentum is transferred to the land surface. Some authors have directly linked z_{0m} of vegetation canopies to leaf area index (e.g., Lindroth, 1993; Raupach, 1994). Surface roughness length is about 10% of canopy height, but this relationship will vary with leaf area density and its vertical distribution (Shaw and Pereira, 1982). We

calculated daily z_{0m} as the average of half-hourly z_{0m}, which we calculated iteratively (Sonnentag et al., 2011) during near-neutral stratification ($|z/L| < 0.025$, where L is the Obukhov's length) and relatively high winds ($u > 1\ m\ s^{-1}$) with:

$$z_{0m} = \frac{z - d_0}{\exp((\kappa) * u/u_*)} \quad (1)$$

where z is the measurement height (3.15 m), d_0 is the zero-displacement height (m), κ is the von Karman constant (0.4), u and u_* are the wind speed ($m\ s^{-1}$) and friction velocity ($m\ s^{-1}$), respectively, both obtained from half-hourly averages of sonic anemometer measurements.

2.3. Digital camera imagery

Digital cameras directly addressable via Internet Protocol ('webcams') provide an easy-to-use ability to build a long-term high-frequency image archive while requiring only little maintenance. In October 2007, we installed an inexpensive indoor webcam (DCS-900; D-Link Corporation, Taipei, Taiwan) in a weatherproof camera house mounted on the tower at a height of 2 m facing west, in the direction of the upwind fetch of the eddy covariance system (Detto et al., 2010). The fixed webcam had a horizontal view of the pepperweed-infested southern part of the site subjected to year-round grazing and mowing. Limited technical specifications for the camera are available online (http://www.dlink.com/products/?pid=270). The webcam was connected to a wired local area network through a router and configured using a web browser. Photographs (680 pixels by 480 pixels = 0.33 mega-pixels) were retrieved from the camera via HTTP every 30 min during daytime between DOY 277 in 2007 and 2010, and stored on a personal computer as uncompressed 24-bit Joint Photographic Experts Group (JPEG) files with color information as DN (0–255, i.e. 8-bit quantization) for *RGB* brightness levels.

We extracted *RGB* brightness levels for two regions-of-interest [ROI]: one covering pepperweed and one covering the light-grey instrumentation pole (as proxy for a white reference needed for the calculation of *CIE Y* with Eq. (5); Poynton, 2003) for reference (ROI_{ref}) (Fig. 1). The ROI was chosen to be representative for the footprint of the eddy covariance system, i.e. for pepperweed subjected to mowing and grazing outside the fenced enclosure (see Fig. 1 in Detto et al., 2010; Sonnentag et al., 2011). The ROI_{ref} was chosen to extract *RGB* brightness for a neutral reference of constant light-grey color.

For each photograph we calculated mean ROI and ROI_{ref} *RGB* brightness levels for further analysis. *RGB* brightness levels varied substantially, mostly in an asymmetrical manner, over the course of the day (Fig. 2). Similar asymmetrical patterns were described in a previous study where the camera was also pointing to the west (Ahrends et al., 2008). In contrast to previous studies using several mid-day images from the same camera (Richardson et al., 2009) or using one solar noon image each from three cameras of the same model (Kurc and Benton, 2010), we calculated daily mean values for *RGB* and RGB_{ref} brightness levels from images taken between 8:00 and 11:00 h local time to reduce the combined effects of changes in illumination intensity, viewing geometry and shadowing on image acquisition. Over this mid-morning time period *RGB* brightness levels were generally at their maximum and essentially stable (Fig. 2).

For the calculation of various *RGB* color indices, we transformed daily *RGB* brightness levels to daily *RGB* chromatic coordinates (*rgb*; Gillespie et al., 1987) with:

$$r = \frac{R}{R+G+B}; \quad g = \frac{G}{R+G+B}; \quad b = \frac{B}{R+G+B} \quad (2)$$

Using *rgb* instead of *RGB* for the calculation of color indices suppresses the influence of illumination intensity contained in *RGB*, thus describing the actual three primary colors red, green and blue (Gillespie et al., 1987; Woebbecke et al., 1995). Calculating *excess green* from *rgb* chromatic coordinates is redundant since *excess green* becomes simply a linear transformation of the green chromatic coordinate. We calculated the following two *rgb* color indices: *green–red ratio* (*grR*; Adamsen et al., 1999) and *red–blue ratio* (*rbR*; Goddijn-Murphy et al., 2009) as:

$$grR = \frac{g}{r} \quad (3)$$

$$rbR = \frac{r}{b} \quad (4)$$

These two *rgb* color indices, *grR*, and *rbR*, were chosen because of their demonstrated sensitivity to certain color changes that we were interested in within the context of pepperweed's complex phenological pattern: the senescence rate of wheat, i.e. the transition from *dark green* to light *yellow–brown* canopy colors (*grR*; Adamsen et al., 1999), and to detect changes in *yellow* substance in shallow coastal waters (*rbR*; Goddijn-Murphy et al., 2009).

Based on daily *RGB* and RGB_{ref} brightness levels, we calculated *CIE Y* to test if the luminous intensity of light reflected from the pepperweed canopy normalized relative to a reference (here, the light-grey instrumentation pole, which ideally would be white; Poynton, 2003) has better performance for tracking z_{0m} and F_A than *rgb* chromatic coordinates or the two color indices. We calculated *CIE Y* as the linearly weighted sum of *RGB* brightness levels with the weights corresponding to the spectral sensitivity of human vision (i.e., highest and lowers over green and blue, respectively, and intermediate over red wavelengths of the electromagnetic spectrum) according to the luminous efficiency function (Poynton, 2003):

$$CIE\ Y = 0.2125\left(\frac{R}{R_{ref}}\right) + 0.7154\left(\frac{G}{G_{ref}}\right) + 0.0721\left(\frac{B}{B_{ref}}\right) \quad (5)$$

For the use of RGB_{ref} in Eq. (5), the different illumination and viewing geometries of pepperweed and RGB_{ref} needed to be accounted for: the canopy top of the pepperweed infestation is approximately horizontal whereas the light-grey instrumentation pole is approximately vertically and facing east toward the webcam (Fig. 1).

We pursued the following simple approach to reconstruct hypothetical horizontal RGB_{ref} (RGB_{ref_horiz}). First, we calculated daily sums ($MJ\ m^{-2}\ d^{-1}$) from half-hourly S_g measured horizontally ($W\ m^{-2}$). Next, we calculated daily solar radiation for a vertical surface facing east (S_{g_vertic}; $MJ\ m^{-2}\ d^{-1}$) following Tian et al. (2001) based on the well-established concepts described by Liu and Jordan (1960) and Revfeim (1978) to calculate daily solar radiation on arbitrarily inclined surfaces (here: vertical and facing east). For each day of our study period (DOY 274 in 2007 to DOY 273 in DOY 2010), we calculated the ratio of S_{g_vertic} to S_g. Finally, we multiplied each of the three components of RGB_{ref} with the inverse of this ratio to approximate daily values of RGB_{ref} levels for a horizontal reference (i.e., RGB_{ref_horiz}).

In the following analysis, we focused on the determination of lagged (daily) relationships between *RGB* color space information (i.e., *RGB* brightness levels, *rgb* chromatic coordinates, *grR*, *rbR*, and *CIE Y*) and z_{0m} and F_A using cross-correlation functions (Box and Jenkins, 1976). Cross-correlation functions allowed us to compare increasingly delayed versions of *RGB* color space information with z_{0m} and F_A to identify lags between changes in *RGB* color space information and changes in z_{0m} and F_A. We interpret the existence of lagged relationships as an indicator for differences in seasonal dynamics between *RGB* color space information and z_{0m} and F_A, and thus as inability to track pepperweed's structural and functional canopy development.

We tested the cross-correlations at each lag-step (day) for significance using a bootstrapping technique (Efron and Tibshirani,

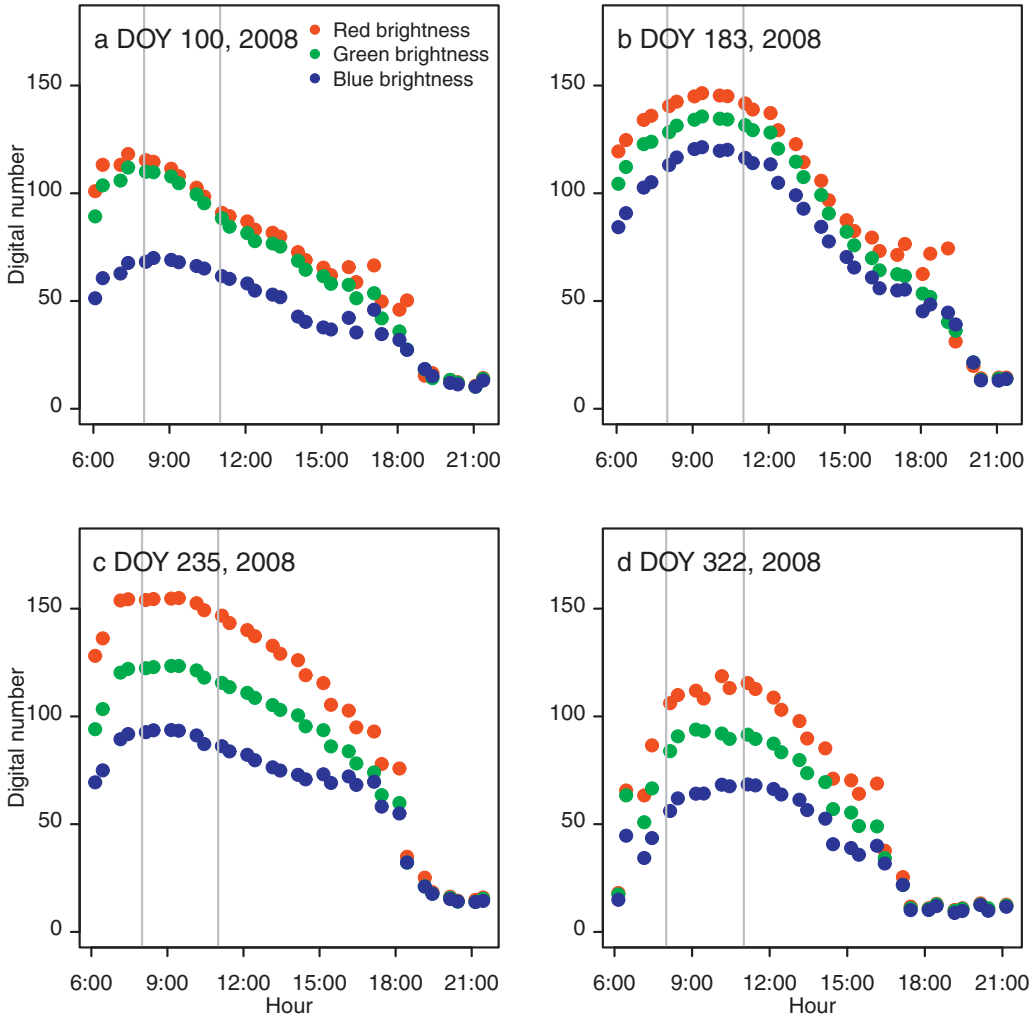

Fig. 2. Diurnal patterns of *RGB* brightness levels for pepperweed (red region-of-interest [ROI] in Fig. 1) at different times of the year. Vertical grey lines indicate the time window (8:00–11:00 am local time) for which daily mean values for *RGB* brightness were calculated.

1993). First, we bootstrapped *RGB* brightness levels, *rgb* chromatic coordinates, *grR*, *rbR*, and *CIE Y* each 1000 times to create 1000 surrogate data sets each. Next, we recalculated the cross-correlation functions between each artificial *RGB* brightness levels, *rgb* chromatic coordinates, *grR*, *rbR*, and *CIE Y* data set and z_{0m} and F_A. Cross-correlations were significant at the 95% level once outside the 0.025 and 0.975 quantiles of the probability density functions for the cross-correlations each obtained with the 1000 surrogate data sets. All analyses were done in the R computing environment (v2.10.0; R Development Core Team, 2009).

3. Results

Seasonal changes in daily z_{0m} were related to changes in pepperweed canopy height and so were associated with plant growth (Fig. 3a): each year z_{0m} peaked in the spring (mid-May) at around DOY 140 during flowering when the plants were fully grown. Daily F_A showed seasonal patterns similar to z_{0m} but with a more pronounced peak that was reached about 15–20 days earlier in late April/early March, while z_{0m} was still increasing (Fig. 3b). Both daily z_{0m} and F_A dropped abruptly in response to the mowing event in 2008 (DOY 137). Toward the end of the years during senescence, F_A declined faster than z_{0m} since biological activity shut down while the plant structure was still present. In a previous study we showed that pepperweed's most prominent key phenological phase (i.e., flowering) together with applied control measures (i.e., mowing) determined our study site's CO_2-source-sink strength: flowering decreased photosynthetic CO_2 uptake but mowing during early flowering reversed these attenuating effects (Sonnentag et al., 2011). In 2009, the year after the mowing event, both z_{0m} and F_A were reduced compared to 2007 and 2008, suggesting decreased pepperweed abundance that at least partially can be attributed to the mowing event. However, in 2010, both z_{0m} and F_A indicate increased pepperweed abundance again. Most remarkable is the growth of a new generation of pepperweed plants toward the end of our study period in 2010 as indicated by the distinct peak in F_A and a minor peak in z_{0m} before the plants senesced.

RGB brightness levels of pepperweed evolved roughly in concert (Fig. 3c), but the fluctuations were most pronounced for red brightness. Generally red > green > blue brightness, except between DOY ~345 (i.e., starting in the previous year) and DOY ~120 when red ≈ green > blue brightness. During this period the site appears green due to green grasses, which are active over the wet winters (DOY ~345–DOY ~70), and green pepperweed during early vegetative growth (DOY ~50–DOY ~120). *RGB* brightness levels reached a mid-year plateau roughly corresponding to pepperweed flowering and seed maturation, and finally declined with senescence. Small differences in the temporal dynamics of *RGB* brightness levels occurred during flowering and seed maturation. For example, at around DOY 200 in 2008, red brightness increased while green and

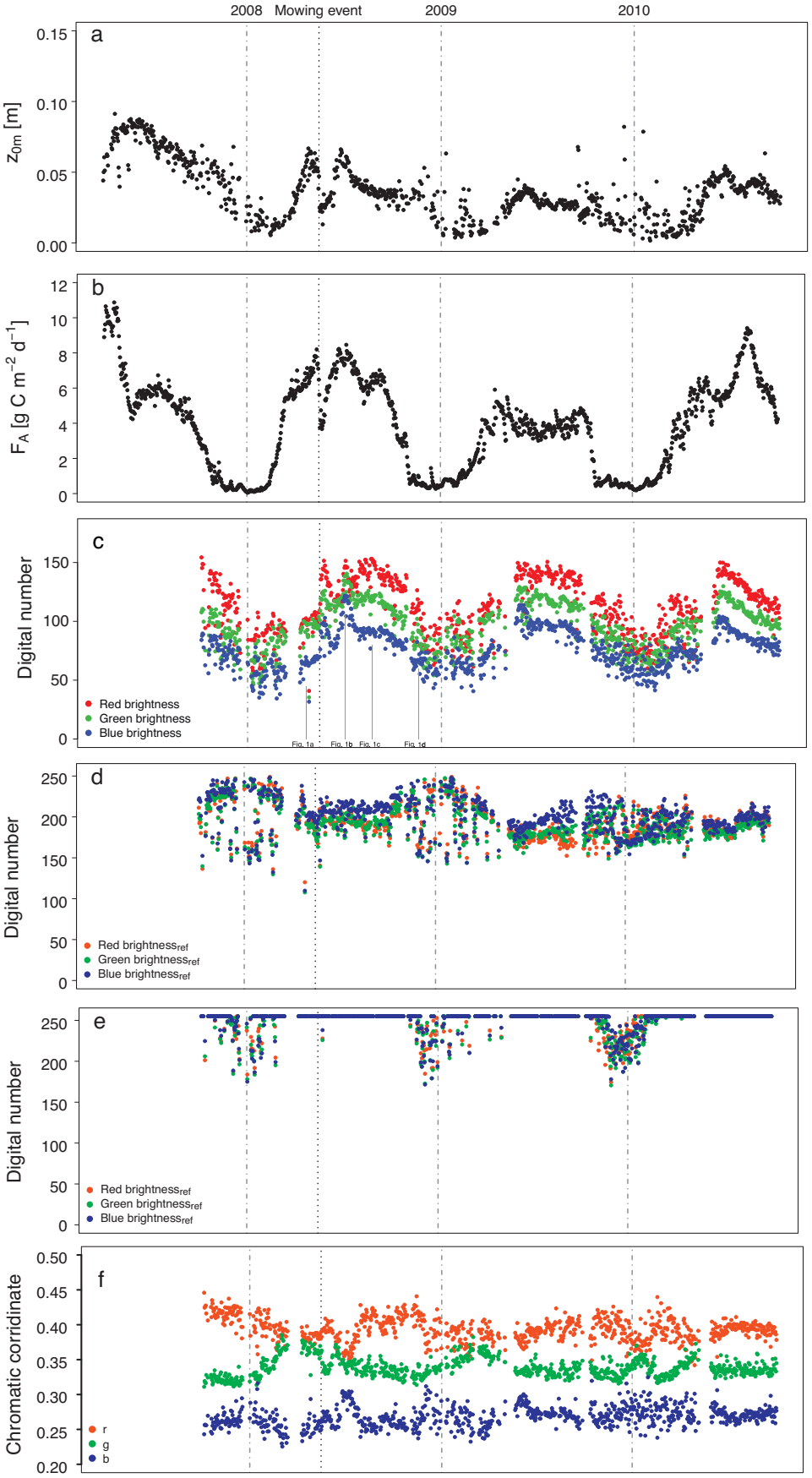

Fig. 3. Seasonal changes in daily (a) surface roughness length (z_{0m}), (b) canopy photosynthesis (F_A), (c) *RGB* brightness levels as digital numbers for pepperweed (red ROI in Fig. 1), (d) *RGB* brightness levels (RGB_{ref}) as digital numbers for the light-grey instrumentation pole (blue ROI in Fig. 1), (e) same as (d) but corrected for vertical illumination ($RGB_{ref,horiz}$), (f) *rgb* chromatic coordinates, (g) *green–red ratio* (*grR*) and *red–blue ratio* (*rbR*), and (h) *relative luminance* (*CIE Y*).

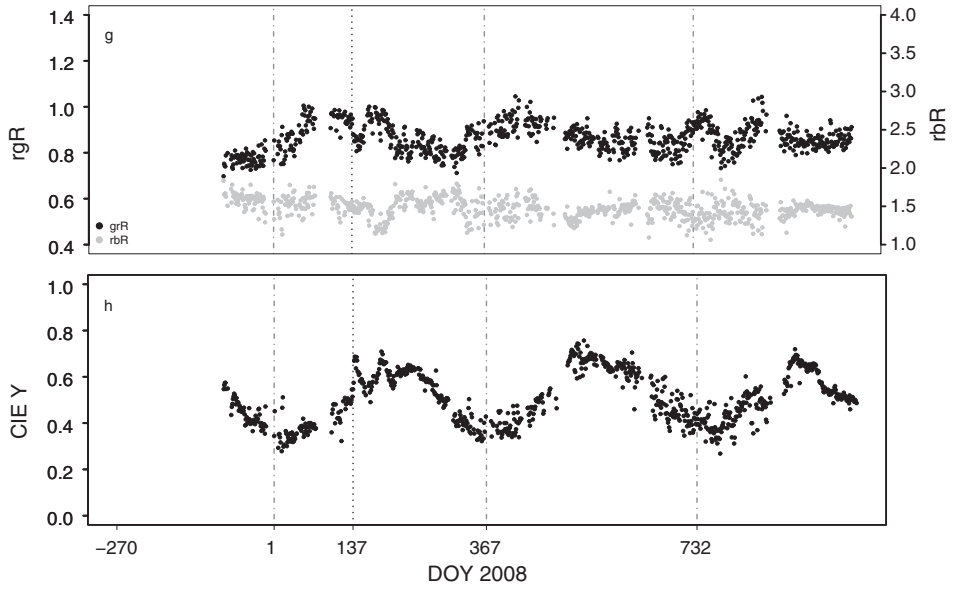

Fig. 3. (*Continued*).

blue brightness decreased. Overall, seasonal changes in *RGB* brightness levels were controlled by the combined effects of changes in illumination intensity and changes in the spectral characteristics associated with canopy color changes according to pepperweed's phenological cycle.

As expected, RGB_{ref} brightness levels were less variable than *RGB* brightness levels with red ≈ green ≈ blue brightness (Fig. 3d). In contrast to *RGB* brightness levels for pepperweed (Fig. 3c), seasonal changes in RGB_{ref} brightness levels were solely caused by changes in illumination intensity due to the Earth's revolution, and not by color changes of the light-grey instrumentation pole. The effect of the instrumentation pole's orientation (∼east) and inclination (∼90°) is evident in the seasonality of RGB_{ref} brightness levels which were higher over the winter months and lower over the summer months. The daily averages were calculated from RGB_{ref} brightness levels between 8:00 and 11:00 am local time. In the winter, the height of the Sun above the horizon is lower, thus the east-facing instrumentation pole was illuminated at higher solar zenith angles over the morning hours than in the summer. Consequently, the illumination intensity and thus RGB_{ref} brightness levels were higher in winter compared to summer. With our simple approach based on the ratio of S_g to $S_{g;horiz}$ (data not shown), we corrected RGB_{ref} brightness levels for orientation and inclination to approximate RGB_{ref_horiz} for use in Eq. (5) (Fig. 3e): over the summer months with the Sun high above the horizon, a hypothetical horizontal instrumentation pole was easily saturated (i.e., RGB_{ref_horiz} = 255:255:255), but had lower RGB_{ref_horiz} values in the winter, and was thus comparable to the seasonality of *RGB* brightness levels for pepperweed (Fig. 3c). Recently, we noticed in a digital camera intercomparison at Harvard Forest that the inexpensive webcam used on Sherman Island tends to saturate easily even under much lower illumination intensities (Oliver Sonnentag, *unpublished data*).

The *rgb* chromatic coordinates provide a more intuitive representation of pepperweed canopy color changes than *RGB* brightness levels (Fig. 3f). In contrast to *RGB* brightness levels, *rgb* chromatic coordinates varied according to color changes as perceived by human vision. For example, the green chromatic coordinate varied in accordance with perceived canopy greenness, which peaked relatively early in the year due to green grasses and green pepperweed during early vegetative growth, i.e. before z_{0m} and F_A (Fig. 3a and b). After reaching a peak (DOY ∼75), the green chromatic coordinate decreased again but did not allow for a further distinction between green and different non-green phases (i.e., between early vegetative growth and flowering), or between non-green phases (i.e., between flowering, seed maturation and senescence). In contrast, the red and blue chromatic coordinates mostly fluctuated during non-green phenological phases, with peaks and valleys corresponding to color changes related to pepperweed flowering, seed maturation or senescence.

Because of its strong dependence on the green chromatic coordinate (Fig. 3g), *grR* showed a similar pattern with increases indicative for site green-up (i.e., green grasses and pepperweed during early vegetative growth) and pepperweed regrowth after mowing in 2008 (Fig. 3f and g). In contrast, fluctuations in *rbR* emphasized structural and functional information carried in the red and blue chromatic coordinates, while removing the site green-up peak reflected in the green chromatic coordinate and *grR* (Fig. 3f and g). Similar to the red and blue chromatic coordinates, *rbR* mostly fluctuated during non-green phenological phases, but without revealing a clear response to either pepperweed flowering or seed maturation or senescence in relation to z_{0m} or F_A. Assuming that our simple approach of normalizing pepperweed *RGB* brightness levels relative to RGB_{ref_horiz} sufficiently removed the effects of seasonal changes in illumination intensity, fluctuations in *CIE Y* synthesize fluctuations in *RGB* brightness levels associated with changes in the spectral characteristics of the pepperweed canopy alone (Fig. 3h).

The 2008 mowing event was captured by an abrupt increase in *RGB* brightness levels and *CIE Y* due to the influence of bright dead grasses and dry soil background after pepperweed was cut (Fig. 3c and h). In contrast, the green chromatic coordinate and *grR* responded to the mowing event with an abrupt decrease (Fig. 3f and g), and no clear response was observed for the red and blue chromatic coordinates and *rbR* (Fig. 3f and g). Neither *RGB* brightness levels nor *rgb* chromatic coordinates nor the color indices nor *CIE Y* showed distinct differences in magnitude in their seasonal patterns between years (Fig. 3c and f–h).

The cross-correlation functions indicate that *RGB* brightness levels, *rgb* chromatic coordinates, the two color indices and *CIE Y* are significantly positively and negatively correlated with z_{0m} and F_A shifted forward and backward over several lags (days to weeks) of different length (Fig. 4a–h). The cross-correlations are generally much weaker for z_{0m} than for F_A, suggesting that color information from webcam imagery appears to be less suited to monitor canopy height and thus structural pepperweed canopy develop-

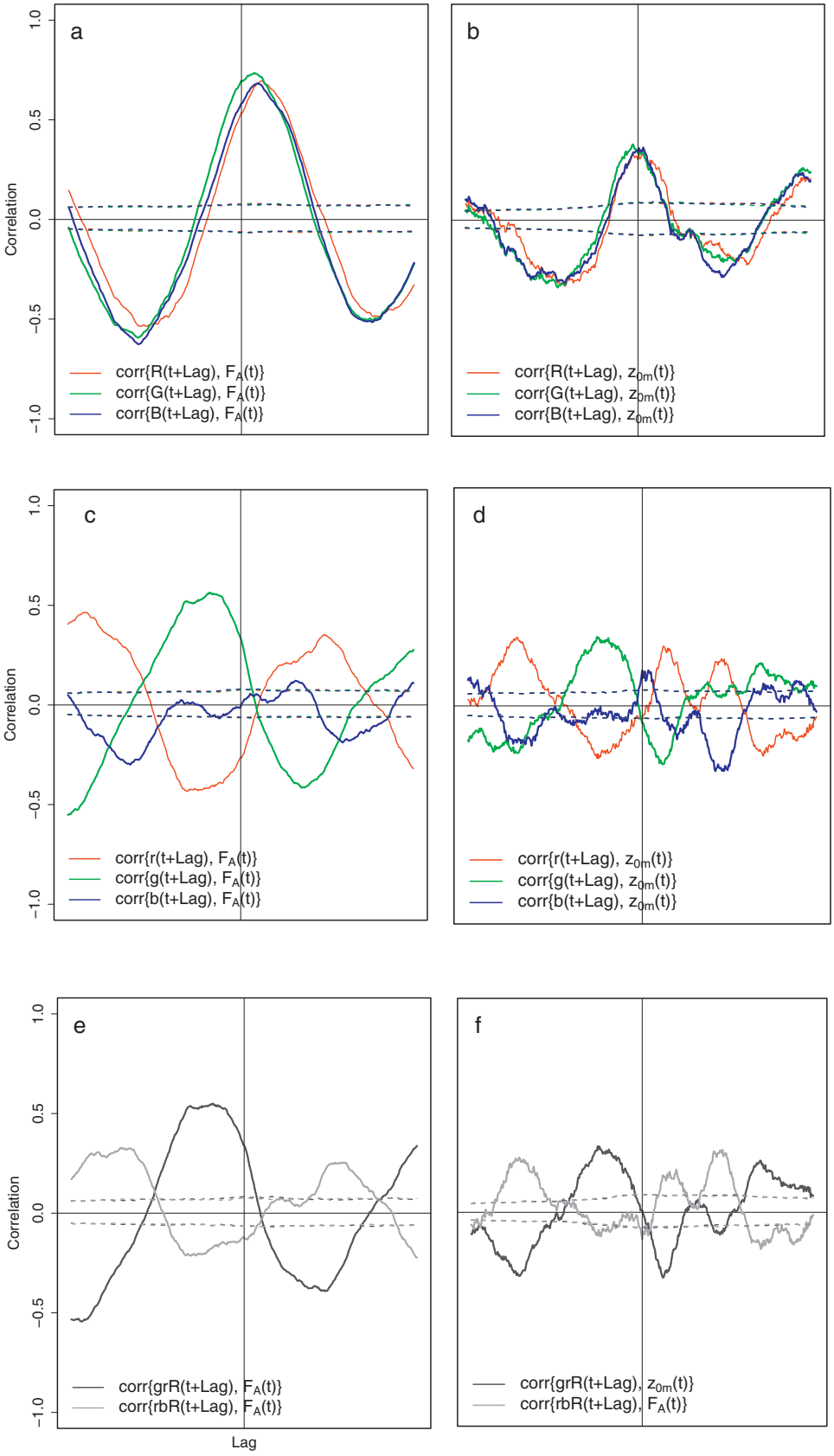

Fig. 4. Cross-correlation functions with a maximum delay of 200 days between *RGB* brightness levels as digital numbers and (a) canopy photosynthesis (F_A) and (b) surface roughness length (z_{0m}), between *rgb* chromatic coordinates and (c) F_A and (d) z_{0m}, *green–red ratio* (*grR*) and *red–blue ratio* (*rbR*) and (e) F_A and (f) z_{0m}, and between *relative luminance* (*CIE Y*) and (g) F_A and (h) z_{0m}. Horizontal dashed lines are the 95% significance levels (obtained with a bootstrapping technique; Efron and Tibshirani, 1993) above/below which cross-correlations were significant.

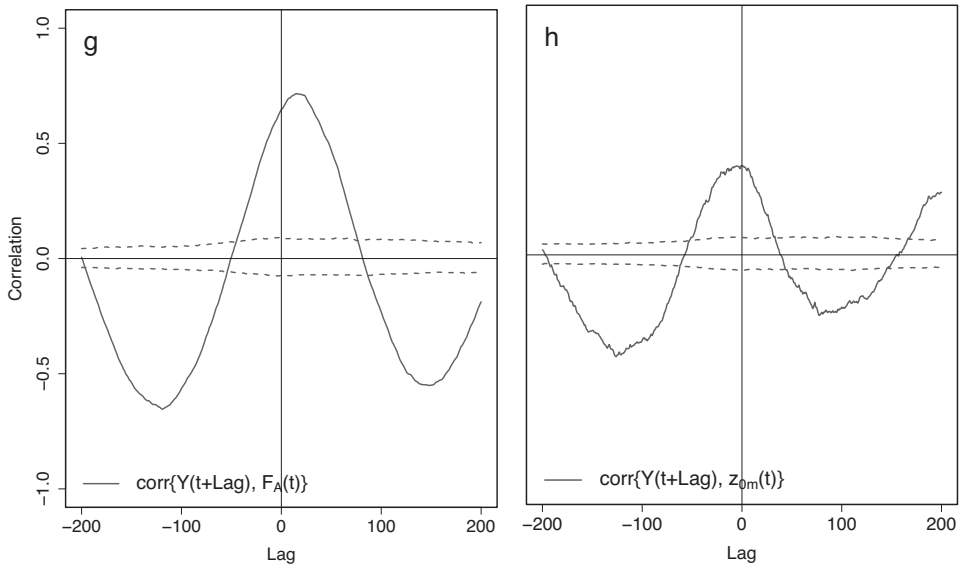

Fig. 4. (*Continued*).

ment (Table 1). As expected from Fig. 3c, the three cross-correlation functions in Fig. 4a and b are characterized by similar patterns, showing high maximum correlations at similar lags of around one and two-three weeks for z_{0m} and F_A, respectively (Table 1).

The cross-correlation functions between *rgb* chromatic coordinates, *grR* and *rbR*, and z_{0m} and F_A show different patterns with maximum or minimum correlations at different lags (Fig. 4c–f; Table 1). Most notably, the cross-correlations for the green chromatic coordinate and *grR* indicate that maximum canopy greenness was reached prior to maximum z_{0m} and maximum F_A, i.e. before the plants were fully grown. Thus, canopy greenness as described by the green chromatic coordinate and *grR* may not be useful indicators for canopy height or photosynthetic activity as described by z_{0m} and F_A, respectively.

The cross-correlation functions between *CIE Y* and z_{0m} and F_A show high correlations at lags closest to zero (Table 1), suggesting that *CIE Y* alone appears to be a suitable indicator to track the structural and functional development of a pepperweed canopy (Fig. 4g and h).

We recalculated the cross-correlation functions after removal of the main trends in all time series by differentiation, and no more significant correlations were observed, i.e. indicating that no relationships other than the seasonal trends exist (data not shown).

Table 1
Maximum (max.) or minimum (min.) correlation coefficients (r) and corresponding lags of the cross-correlation series (Fig. 3a–h) between *RGB* brightness levels encoded as digital numbers (DN), *rgb* chromatic coordinates, *green–red ratio* (*grR*), *red–blue ratio* (*rbR*), and *relative luminance* (*CIE Y*) and surface roughness length (z_{0m}) and canopy photosynthesis (F_A).

	F_A		z_{0m}	
	Max. r or min. r	Lag (days)	Max. r or min. r	Lag (days)
Red	0.69	24	0.33	6
Green	0.72	17	0.37	−6
Blue	0.68	19	0.36	6
Red	0.46	−179	0.34	−144
Green	0.56	−36	0.34	−52
Blue	−0.30	−128	−0.32	84
grR	0.55	−36	0.33	−52
brR	0.33	−143	0.34	94
CIE Y	0.72	15	0.36	−5

4. Discussion

Previous studies have demonstrated that red, green and blue, *RGB*, color space information from repeated horizontal or oblique landscape photographs can be used to monitor functional changes (e.g., F_A) of vegetation canopies based on canopy greenness as described by color indices (e.g., Ahrends et al., 2008; Graham et al., 2010a; Kurc and Benton, 2010; Richardson et al., 2007, 2009). Most of these ecosystem-scale studies used *excess green* or the green chromatic coordinate in ecosystems that experienced natural, undisturbed phenological cycles such as deciduous forests in Europe and the United States (e.g., Ahrends et al., 2009; Richardson et al., 2007, 2009). For these sites, canopy greenness can be considered as representative for the functional state of the ecosystem: increasing and decreasing canopy greenness is indicative for the increasing and decreasing amount of photosynthetically active green leaves in the spring and during fall, respectively.

The opposite is the case for canopies with a complex phenological pattern such as that of our pepperweed-infested study site on Sherman Island. A color index such as *rbR* or the red and blue chromatic coordinates may emphasize specific non-green phenological phases of pepperweed alone (e.g., flowering/seed maturation). In contrast, the temporal dynamics of the green chromatic coordinate and *grR* were governed by ecosystem-scale color changes induced by pepperweed's plant physiological features (i.e., the transition from dark-green basal rosette leaves to grey-green stem leaves) in combination with background materials (i.e., green grasses active during the winter and early spring when pepperweed plant growth starts with the occurrence of dark-green basal rosette leaves). The existence of lagged relationships indicates that the *rgb* chromatic coordinates and the two color indices failed to track z_{0m} and F_A. Thus, none of these indicators for seasonal changes in canopy color were representative for the temporal dynamics of either z_{0m} or F_A, therefore limiting their capacity to infer the structural or functional state of the pepperweed-infested pasture. Ideally, *RGB* color space information suitable for that purpose is related to z_{0m} and F_A with lag = 0.

The color information provided by 24-bit JPEG photographs with 8-bit quantization is *RGB* brightness levels encoded as DN (0–255), spanning overlapping wavelength ranges located approximately between 400 and 700 nm. The exact *RGB* wavelength ranges are not available to the end-user of commercially available digital cameras

or webcams. Over the course of a day, changes in *RGB* brightness levels are controlled by various non-varying and varying factors including the spectral characteristics of the target material and illumination intensity, respectively. However, seasonally, the temporal dynamics of *RGB* brightness levels at least partly reflected ecosystem-scale changes in spectral characteristics through color changes of the pepperweed canopy (Fig. 3c).

For the calculation of *relative luminance*, *CIE Y*, with Eq. (5) we used a simple but innovative approach to construct hypothetical horizontal RGB_{ref}, RGB_{ref_horiz}, based on separately measured incoming solar radiation, S_g. By calculating *CIE Y* we removed or at least greatly suppressed the influence of changes in illumination intensity, thus we attribute seasonal changes in *CIE Y* to changes in spectral characteristics, and thus brightness, of the pepperweed canopy top alone. With the onset of flowering and the following seed maturation, the pepperweed canopy became brighter than during early vegetative growth and during senescence, causing *CIE Y* to reflect temporal dynamics that correspond to pepperweed plant growth and photosynthetic activity. Thus, we advocate the use of *CIE Y* obtained from high-frequency image archives, which might be useful to make informed decision regarding the timing of pepperweed control measures such as mowing. The timing of pepperweed mowing is important for its effectiveness and it determines the infestation's CO_2 sink-source strength (e.g., Renz and DiTomaso, 2004, Sonnentag et al., 2011).

In contrast, *CIE Y* cannot be considered as useful to assess the effectiveness of different pepperweed control measures. Seasonal changes in *CIE Y* were largely controlled by the spectral characteristics and resulting brightness of the canopy top and are not influenced by the amount of photosynthetically active pepperweed biomass underneath. As a result, *CIE Y* mainly tracked the seasonality of z_{0m} and F_A of the first generation of pepperweed plants each year but failed to capture their different magnitudes (Fig. 3a, b and h).

The findings of our study lead to a series of questions. For example, is *RGB* color space information from digital camera imagery generally able to capture interannual variability in F_A? To date, no study has systematically examined the consistency of *RGB* color space information from different digital cameras over time and across sites, thus how well do color changes as tracked with color indices calculated from *RGB* color space information capture interannual variability in F_A? Can color indices obtained from different digital cameras at different sites capture intersite differences in F_A? Are intersite differences in orientation and view angle and especially digital camera choice critical issues in such synthesis activities? For example, one caveat of inexpensive, consumer-grade indoor webcams such as the D-Link DCS-900 used for our study is that their low-resolution photographs are often of low quality (i.e., characterized by relatively low sharpness, high noise, low contrast, poor color balance) compared to higher quality photographs used in previous phenological studies based on digital repeat photography (e.g., Ahrends et al., 2008). Thus, given the wide range of options for digital repeat photography, are different digital cameras in agreement regarding their phenological information content obtained from *RGB* brightness levels despite these differences in image quality?

With our study we provide an example for the use of multi-year image archives for phenological research that goes beyond commonly used color indices calculated from *RGB* color space information alone. Given the limited numbers of possible combinations of individual *RGB* brightness levels or *rgb* chromatic coordinates, we believe that the real potential of digital image archives for phenological and other environmental research lies in their coupled use with related environmental measurements such as S_g. For example, a recent study combined infrared thermometer measurements, a sunfleck model of soil surface temperature with digital camera imagery to calculate soil surface and subsurface temperature variations across a forest floor (Graham et al., 2010b).

At the same time, our study highlights some limitations of digital image archives specifically for phenological research (here, failure of *CIE Y* to capture the magnitude and thus interannual differences in F_A), which need to be addressed in a systematic manner in the future with image archives from various sites and different digital cameras. Thus, we strongly encourage the research community to be creative and cautious regarding the phenological information that can be retrieved from *RGB* brightness levels alone, especially when working with complex phenological patterns where the dynamics of a specific color index might not be representative for structural or functional canopy development.

5. Conclusions

For this study we analyzed a three-year low-quality image archive obtained from a webcam overlooking a pepperweed-infested pasture in conjunction with eddy covariance measurements to explore the usefulness of *RGB* color space information in its ability to track peppweeed's structural and functional canopy development. Based on cross-correlation functions between *RGB* color space information and z_{0m} and F_A, we conclude:Widely used color indices such as *grR* and *rbR*, and *rgb* chromatic coordinates fail to track pepperweed canopy development due to the plant's complex phenological pattern: color changes as tracked by color indices are not representative for the structural and functional state of the canopy.Taking into account changes in illumination intensity, *relative luminance*, *CIE Y*, can be calculated from *RGB* color space information, which for pepperweed appears to be a better indicator for z_{0m} and especially for F_A, and thus may serve as an aid for making informed decisions regarding the timing of applied control measures but not for the assessment of their effectiveness.

Surprisingly, despite the numerous possibilities for repeat photography resulting in image archives consisting of landscape photographs of varying quality, no study to date has addressed the issue of image quality for the continuous monitoring of vegetation status. As a consequence, we cannot draw conclusions regarding the influence of image quality, and thus digital camera choice, on our results.

Acknowledgements

We thank Marek Jakuboskwi (University of California Berkeley) for helpful discussions during the preparation of this manuscript. We also thank Ted Hehn and Joseph Verfaillie for their dedicated support in conducting the field measurements and servicing the instruments. We thank the two anonymous reviewers for their constructive comments that substantially improved the manuscript. This study was funded by National Science Foundation grant number ATM-0628720.

References

Adamsen, F.J., Pinter Jr., P.J., Barnes, E.M., LaMorte, R.L., Wall, G.W., Leavitt, S.W., Kimball, B.A., 1999. Measuring wheat senescence with a digital camera. Crop Sci. 39, 719–724.

Adamsen, F.J., Coffelt, T.A., Nelson, J.M., Barnes, E.M., Rice, R.C., 2000. Method for using images from a color digital camera to estimate flower number. Crop Sci. 40, 704–709.

Ahrends, H.E., Brugger, R., Stockli, R., Schenk, J., Michna, P., Jeanneret, F., Wanner, H., Eugster, W., 2008. Quantitative phenological observations of a mixed beech forest in northern Switzerland with digital photography. J. Geophys. Res.: Biogeo. 113, 11.

Ahrends, H.E., Etzold, S., Kutsch, W.L., Stoeckl, R., Bruegger, R., Jeanneret, F., Wanner, H., Buchmann, N., Eugster, W., 2009. Tree phenology and carbon dioxide fluxes: use of digital photography for process-based interpretation at the ecosystem scale. Climate Research 39, 261–274.

Andrew, M.E., Ustin, S.L., 2008. The role of environmental context in mapping invasive plants with hyperspectral image data. Remote Sens. Environ. 112, 4301–4317.
Baldocchi, D.D., 2003. Assessing the eddy covariance technique for evaluating carbon dioxide exchange rates of ecosystems: past, present and future. Glob. Change Biol. 9, 479–492.
Box, G.E.P., Jenkins, G.M., 1976. Time Series Analysis: Forecasting and Control. Holden Day, San Francisco.
Cheng, H.D., Jiang, X.H., Sun, Y., Wang, J., 2001. Color image segmentation: advances and prospects. Pattern Recogn. 34, 2259–2281.
Detto, M., Baldocchi, D.D., Katul, G.G., 2010. Scaling properties of biologically active scalar concentration fluctuations in the surface boundary layer over a managed peatland. Bound.-Lay. Meteorol. 136, 407–430.
Efron, B., Tibshirani, R.J., 1993. An Introduction to the Bootstrap. Chapman & Hall, New York.
Francis, A., Warwick, S.I., 2007. The biology of invasive alien plants in Canada. 8. *Lepidium latifolium* L. Can. J. Plant Sci. 87, 639–658.
Garrity, S.R., Vierling, L.A., Bickford, K., 2010. A simple filtered photodiode instrument for continuous measurement of narrowband NDVI and PRI over vegetated canopies. Agric. Forest Meteorol. 150, 489–496.
Gillespie, A.R., Kahle, A.B., Walter, R.E., 1987. Color enhancement of highly correlated images. II. Channel ratio and "chromaticity" transformation techniques. Remote Sens. Environ. 22, 343–365.
Goddijn-Murphy, L., Dailloux, D., White, M., Bowers, D., 2009. Fundamentals of *in-situ* digital camera methodology for water quality monitoring of coast and ocean. Sensors 9, 5825–5843.
Godoy, O., Richardson, D.M., Valladares, F., Castro-Diez, P., 2009. Flowering phenology of invasive alien plant species compared with native species in three Mediterranen-type ecosystems. Ann. Bot. (Lond.) 103, 485–494.
Graham, E.A., Riordan, E.C., Yuen, E.M., Estrin, D., Rundel, P.W., 2010a. Public internet-connected cameras used as a cross-continental ground-based plant phenology monitoring system. Glob. Change Biol. 16, 3014–3023.
Graham, E.A., Lam, E.A., Yuen, E.M., 2010b. Forest understory soil temperatures and heat flux calculated using a Fourier model and scaled using a digital camera. Agric. Forest Meteorol. 150, 640–649.
Jacobs, N., Burgin, W., Fridrich, N., Abrams, A., Miskell, K., Braswell, B. H., Richardson, A. D., Pless, R., 2009. The global network of outdoor webcams: properties and applications. Proceedings ACM GIS '09 (November 4–6, 2009. Seattle, WA, USA), 111–120.
Lindroth, A., 1993. Aerodynamic and canopy resistance of short-rotation forest in relation to leaf area index and climate. Bound.-Lay. Meteorol. 66, 265–279.
Kurc, S.A., Benton, L.M., 2010. Digital image-derived greenness links deep soil moisture to carbon uptake in a creosotebush-dominated shrubland. J. Arid Environ. 74, 585–594.
Liu, B.Y.H., Jordan, R.C., 1960. The interrelationship and characteristic distribution of direct, diffuse and total solar radiation. Sol. Energy 4, 1–19.
Meyer, G.E., Camargo Neto, J., 2008. Verification of color vegetation indices for automated crop imaging applications. Comput. Electron. Agric. 63, 282–293.
Monteith, J.L., Unsworth, M.H., 1990. Principles of Environmental Physics. Edward Arnold, London.
Perez, A.J., Lopez, F., Benlloch, J.V., Christensen, S., 2000. Color and shape analysis techniques for weed detection in cereal fields. Comput. Electron. Agric. 25, 197–212.
Poynton, C., 2003. Digital Video and HDTV: Algorithms and Interfaces. Morgan Kaufmann Publishers, San Francisco.
Raupach, M.R., 1994. Simplified expressions for vegetation roughness length and zero-displacement as functions of canopy height and area index. Bound.-Lay. Meteorol. 71, 211–216.
R Development Core Team, 2009. R: A Language and Environment for Statistical Computing. R Foundation for Statistical Computing, Vienna, ISBN: 3-900051-07-0. http://www.R-project.org.
Renz, M.J., DiTomaso, J.M., 2004. Mechanism for the enhanced effect of mowing followed by glyphosate application to resprouts of perennial pepperweed (*Lepidium latifolium*). Weed Science 52, 14–23.
Revfeim, K.J.A., 1978. A simple procedure for estimating global daily radiation on any surface. J. Appl. Meteorol. 17, 1126–1131.
Richardson, A.D., Jenkins, J.P., Braswell, B.H., Hollinger, D.Y., Ollinger, S.V., Smith, M.L., 2007. Use of digital webcam images to track spring green-up in a deciduous broadleaf forest. Oecologia 152, 323–334.
Richardson, A.D., Braswell, B.H., Hollinger, D.Y., Jenkins, J.P., Ollinger, S.V., 2009. Near-surface remote sensing of spatial and temporal variation in canopy phenology. Ecological Applications 19, 1417–1428.
Ryu, Y., Baldocchi, D.D., Ma, S., Falk, M., Verfaille, J., Hehn, T., Sonnentag, O., 2010a. Testing the performance of a novel spectral reflectance sensor, built with light emitting diodes (LEDs), to monitor ecosystem metabolism, structure and function. Agric. Forest Meteorol. 150, 1597–1606.
Ryu, Y., Nilson, T., Kobayashi, H., Sonnentag, O., Law, B.E., Baldocchi, D.D., 2010b. On the correct estimate of leaf area index: does it reveal information on clumping effects? Agric. Forest Meteorol. 150, 463–472.
Shaw, R.H., Pereira, A.R., 1982. Aerodynamic roughness of a plant canopy: a numerical experiment. Agric. Meteorol. 26, 51–65.
Sonnentag, O., Detto, M., Runkle, B.R.K., Teh, Y.A., Silver, W.L., Kelly, M., Baldocchi, D.D., 2011. Carbon dioxide exchange or a pepperweed (*Lepidium latifolium* L.) infestation: how do flowering affect canopy photosynthesis and autotrophic respiration? J. Geophys. Res.: Biogeo., doi:10.1029/2010JG001522.
Tian, Y.Q., Davies-Colley, R.J., Gong, P., Thorrold, B.W., 2001. Estimating solar radiation on slopes of arbitrary aspect. Agric. Forest Meteorol. 109, 67–74.
Woebbecke, D.M., Meyer, G.E., Von Bargen, K., Mortensen, D.A., 1995. Color indices for weed identification under various soil, residue, and lightning conditions. Trans. ASAE 38, 259–269.
Wolkovich, E.M., Cleland, E.C., 2010. The phenology of plant invasions: a community ecology perspective. Front Ecol. Environ., doi:10.1890/100033.
Young, J.A., Turner, C.E., James, L.F., 1995. Perennial pepperweed. Rangelands 17, 121–123.